ASTRONOMY & ASTROPHYSICS
SUPPLEMENT SERIES

Astron. Astrophys. Suppl. Ser. **126,** 91-103 (1997)

Spectroscopic and photometric behaviour of the FU Orionis variable Z Canis Majoris⋆

M. Teodorani[1], L. Errico[1], A.A. Vittone[1], F. Giovannelli[2], and C. Rossi[3]

[1] Osservatorio Astronomico di Capodimonte, Via Moiariello 16, I-80131 Napoli, Italy
[2] Istituto di Astrofisica Spaziale, CNR, Via E.Fermi 21, C.P. 67, I-00044 Frascati (Roma), Italy
[3] Istituto Astronomico, Universita' "La Sapienza" di Roma, Via Lancisi 29, I-00161 Roma, Italy

Received July 25, 1996; accepted March 3, 1997

Abstract. We present optical and IR photometry, optical multi-dispersion spectroscopy, and IR spectrophotometry of the FU Ori variable Z Canis Majoris, obtained in the years 1984, 1985, 1989 and 1996. A comparison of data obtained in 1984 and 1985 confirms that in 1985 Z CMa underwent a low-power eruption. The enhancement of Hα emission line, the transition of Hβ and Fe II lines from pure absorption to emission with or without a P Cygni profile, the appearance of the He I 6678 Å absorption line, a radial velocity increase of about 30% of the P Cygni absorption components, and finally a $0.2-0.3$ mag increase of IR luminosity, were all dinstinctive characteristics of this state. Further observations in 1996 show that Z CMa is in a low-luminosity state at $V = 10.24$ while the appearance of a double-peaked Hα emission, with the blue component much weaker than the red one, is the most significant spectroscopic variation. Energy distributions in the range $0.4-5$ μm, obtained during 1984 and 1985 observational runs, are also presented.

Key words: stars: individual: Z CMa — stars: pre-main-sequence — stars: Be — stars: variables: other

1. Introduction

Z CMa is a variable luminous pre-main-sequence object. Although Z CMa is normally classified as an Herbig Ae/Be star, it has many features in common with FU Ori variables (Hartmann et al. 1989). The FU Ori variables are pre-main-sequence objects associated with curved reflection nebulosity that have undergone large, decade-long photometric outbursts. Their spectra vary from F or G supergiant spectral type in the optical region to M in the near-infrared and show large infrared excesses and signs of strong mass-outflow. Doubled absorption line profiles are observed in many FU Ori objects. Z CMa is associated with a curved reflection nebulosity (Bhatt & Sagar 1992) and a high-velocity optical jet-like outflow with a linear extent of 3.6 pc (Poetzel et al. 1989). In the past, Z CMa showed irregular optical variability from a *quiescent* state at $V = 11.5$ to an *active* state at $V = 8.5$ (Covino et al. 1984; Hessman et al. 1991). A 0.4 mag eruption and a 0.7 mag outburst occurred in 1985 and 1987 respectively, were observed and well studied (Hessman et al. 1991). More recently Z CMa reached in 1992 a low state at $V = 10.50$ (Miroshinenko et al. 1993). Moreover, it is possible that irregular variations mask regular variations produced by the modulation of an inhomogeneous spot-like photosphere due to axial rotation of the star (Herbst et al. 1987). Photometric variations of the order of $0.1-0.2$ mag on a scale of $2-3$ days are also present (Covino et al. 1984) and it seems that they are strictly connected with the active state of the star.

The spectrum of Z CMa is a superposition of a spectrum from a rotating middle F star with that of a late B star with P Cygni Balmer lines (Strom et al. 1972) but, with the exception of the He I 6678.15 Å line, seldom detected (Herbig 1960; Covino et al. 1984; Hartmann et al. 1989; Hessman et al. 1991), there is no convincing evidence of any He I absorption which should be expected from a B-type photosphere.

The most prominent spectroscopic features and their variability are explained by the presence of a circumstellar disk with a high accretion rate. The disk axis was recently estimated to have an inclination $i = 56°$ (Poetzel et al. 1989; Hessman et al. 1991). In particular, three very distinguished spectroscopic effects were observed: accretion-driven disk absorption lines, accretion-driven disk emission lines and wind-driven strong P Cygni lines.

The disk-driven absorption line signature (Hartmann et al. 1989; Welty et al. 1992) comes from the presence of double-peaked absorption-line profiles with a velocity

Send offprint requests to: A.A. Vittone

⋆ Based on observations collected at the European Southern Observatory in La Silla, Chile.

difference of 100 km s^{-1} or more, most common longward of 5800 Å, as expected from a disk rotating at Keplerian velocities and whose vertical gravity produces a spectrum consistent with that of a low-gravity atmosphere. This relevant occurrence has been strongly suggested by the comparison of the observed lines with model disk spectra synthesized from supergiant spectra of standard stars (Welty et al. 1992). It is also possible to confirm the disk-driven absorption line doubling effect by cross-correlating Z CMa spectra with spectra of giants as templates (Hartmann et al. 1989). Moreover observations by Welty et al. (1992) confirm a theoretically predicted correlation between rotational velocity $v \sin i$ and wavelength, in the framework of a disk model in which the temperature rises toward the internal region of a disk in the Keplerian regime of motion. All these effects, relative to absorption lines, are proof of an internally heated object, consistent with the inner zone of an optically thick accretion disk where most of the energy is generated near the midplane.

The observed emission lines, mostly from neutral and singly ionized metals, are particularly strong longward of 7000 Å. These lines cannot be formed in the stellar atmosphere, as any line emission from the central star should not be detectable against the background of the disk emission. They can arise from the outer region of the accretion disk at disk radii at least $2-4$ times larger than those at which double absorption profiles are produced, as their rotational width in all states is a factor $1.5-2.0$ smaller than the peak-to-peak separation of the double absorption lines (Hessman et al. 1991; Welty et al. 1992). A very low opacity in the external region of the disk can be the origin of emission line formation. Strong emission features in the spectrum of Z CMa are particularly present in the high states of the star.

The observed P Cygni effects (Covino et al. 1984; Welty et al. 1992; Hartmann & Calvet 1995), particularly prominent shortward of 7000 Å and sometimes with doubled emission, are clear evidence of very strong winds, with terminal velocities of over 1000 km s^{-1}. These winds cannot form in the star photosphere, but may be triggered directly from the inner rapidly rotating region of the accretion disk and probably carry away large amounts of angular momentum from the system. The strong P Cygni effect often present in the spectrum of Z CMa is consistent with mass outflow with a rate of $\dot{M} = 10^{-5}\ M_{\odot}\ \mathrm{yr}^{-1}$ (Croswell et al. 1987). P Cygni Balmer lines are an almost constant feature (Pickering 1913; Merrill 1927), both in the active and in the quiescent state of the star. During the active states, a P Cygni effect is also present in Ca II, Ti II, Na I and Fe II lines and becomes much stronger in the Balmer lines (Hessman et al. 1991) with a sharp increase of both the equivalent width of the emission component and the radial velocity of the absorption component.

There is clear evidence that the inner, absorption-line region and the outer, emission-line region are dynamically, directly or indirectly, coupled by a not yet understood physical process (Hessman et al. 1991). This can be clearly noticed in the high photometric states of Z CMa ($V = 8.5$) in which there is an increase of both the emission line widths and the separation of the double absorption lines, thus suggesting that the maximum luminosity is related to a shrinkage process of both the optically thick and the optically thin disk regions. This process, which is also accompanied by a strong increase of wind-driven P Cygni lines and which culminates in strong outbursts with an increase of over 2 mag and a $60-100$ days duration, can be reasonably due to the occurrence of extremely rapid accretion events, in analogy with other accreting systems like dwarf novae.

Z CMa is also characterized by a strong infrared excess (Oudmaijer et al. 1992; Berrilli et al. 1992), larger than the one predicted by steady accretion disk models and possibly caused by a large, non-spherically symmetric dust cloud surrounding the star, which absorbs light generated from interior regions and reemits this energy in the infrared. A possible correlation of infrared excess with emission lines is suggested by Hamann & Persson (1992), Natta et al. (1993), Torres et al. (1995).

Near-infrared speckle observations of Z CMa reveal it to be a double star with separation $0\farcs1$ at PA = 120°. The north-west component is an infrared object whose broadband spectrum is reminiscent of the infrared companions to several T Tauri stars. The south-east component has the spectral energy distribution expected for a circumstellar disk whose luminosity is dominated by gravitational accretion (Koresko et al. 1991).

In this paper we give the results of the analysis of our photometric observations, of our low, medium and high dispersion spectroscopic observations and of our IR spectrophotometric and photometric observations of Z CMa. We present the mean features of three well distinguished states of this star: a semi-quiescent state in 1984 with much weaker emission features in Fe II lines and with no P Cygni effect in Hβ and Hδ, a semi-active state in 1985 with the presence of strong emissions and P Cygni effects in Balmer and Fe II lines, a similar semi-quiescent state in 1989 and finally a new state in 1996 characterized by the presence of [O I], [S II] emission lines and of a double-emission feature at Hα.

2. Observations and data reduction

Optical and IR observations were performed at La Silla, Asiago and Loiano Observatories in 1984–1985, 1989 and 1996 respectively, at different telescopes.

2.1. Optical photometry

CCD UBV photometric observations were carried out on January 17, 1996 at Loiano 1.52 m telescope with the BFOSC (Bologna Faint Object Spectrograph and

Camera) used in camera mode. BD − 111763 ($V = 8.96$) and BD − 111761 ($V = 9.28$) were used as standard stars.

The data were reduced using specific photometric routines of the ESO MIDAS software.

2.2. Optical spectroscopy

Low, medium and high-dispersion spectroscopy was performed using different telescopes from April 1984 to January 1996. The journal of observations is presented in Table 1.

2.2.1. Low resolution

In April 1984 and March-April 1985 we obtained 33 low dispersion spectra at the ESO 1.52 m telescope equipped with a Boller & Chivens spectrograph + IDS (Image Dissector Scanner) detector with different reciprocal dispersions. 22 spectra were secured in order to detect variability on timescales of seconds and minutes. More recently, in January 1996, we obtained a spectrum at the Loiano 1.52 m telescope equipped with the BFOSC + CCD detector.

IDS spectra were calibrated in flux and wavelength using the IHAP software. Subsequently they were analyzed using the MIDAS software both for continuum normalization and for the determination of spectral line parameters. The BFOSC spectrum was wavelength-calibrated, normalized to the continuum and analyzed by MIDAS software.

Table 1. Journal of optical spectroscopic observations

#	Date	Exp. (s)	Wavelength (Å)	Dispersion (Å mm^{-1})	
1	1984 Apr. 13	240	4720–7098	114	IDS
2	1984 Apr. 14	480	3980–5200	59	IDS
3	1984 Apr. 15	480	4810–6039	59	IDS
4–18	1984 Apr. 16	120	4200–8500	224	IDS
19–25	1984 Apr. 17	120	4200–8500	224	IDS
26	1985 Mar. 15	240	4705–7085	114	IDS
27	1985 Mar. 15	7200	6538–6589	3.0	CES
28	1985 Mar. 16	600	4000–5160	60	IDS
29	1985 Mar. 16	5400	5861–5908	2.6	CES
30	1985 Mar. 17	120	4200–8800	224	IDS
31	1985 Apr. 8	600	3950–5160	60	IDS
32	1985 Apr. 8	7200	6538–6588	3.0	CES
33	1985 Apr. 9	600	4790–7193	114	IDS
34	1985 Apr. 9	9000	6538–6589	3.0	CES
35	1985 Apr. 10	480	4790–8350	224	IDS
36	1985 Apr. 10	9000	8485–8555	3.8	CES
37	1985 Apr. 11	900	5710–6760	3.0	CASPEC
38	1989 Oct. 22	1800	6513–6603	10.4	RES
39	1989 Oct. 23	3000	4820–5020	7.5	RES
40	1996 Jan. 17	600	3940–7860	220	BFOSC
41	1996 Jan. 17	2400	5100–9800	22	BFOSC

Table 2. Journal of IR spectrophotometric observations

#	Date	Exposure		Wavelength
		Wheel (s)	Filter (s)	(μm)
1	1984 Apr. 17	2040	45	1.4 − 2.6
2	1984 Apr. 18	1483	45	2.4 − 4.5
3	″	402	45	4.3 − 5.3
4	1985 Mar. 17	1283	32	1.4 − 2.6
5	″	1125	32	2.4 − 4.5
6	″	268	32	4.3 − 5.3
7	1985 Mar. 18	1246	32	1.4 − 2.6
8	″	1134	32	2.4 − 4.5
9	″	268	32	4.3 − 5.3
10	1985 Apr. 10	1453	32	1.4 − 2.6
11	″	1224	32	2.4 − 4.5

Table 3. UBV photometry obtained with BFOSC + CCD on 1996 January 17

Filter	J.D.	Mag	Exp. (s)
U	2450100.4780	11.78 ± .04	600
B	2450100.4910	11.24 ± .04	300
V	2450100.4976	10.24 ± .01	120

2.2.2. High and medium resolution

In March and April 1985 five high-dispersion spectra were obtained at the ESO 1.4 m CAT (Coudé Auxiliary Telescope) telescope with CES (Coudé Echelle Spectrometer) spectrograph equipped with a Reticon detector and one high-dispersion spectrum was secured at the ESO 3.6 m telescope with CASPEC (Echelle Cassegrain Spectrograph) spectrograph equipped with a CCD detector.

Exposures ranging from 1.5 to 2.5 hours were employed for CES spectra, while a 15 minute exposure was used for CASPEC spectrum. The spectra were reduced with IHAP and/or MIDAS software packages.

In October 1989 three medium-dispersion spectra were secured at the 1.82 m Asiago telescope with RES (Reosc Echelle Spectrograph) spectrograph equipped with a CCD detector. Exposures ranging from 30 minutes to 50 minutes were employed.

The RES echelle orders were straightened through dedicated software developed at the Astronomical Observatory of Capodimonte; in a further stage the spectra were calibrated in wavelength, normalized to the continuum and analyzed using the MIDAS software.

In January 1996 we obtained one medium-dispersion spectrum with an echelle grism at the BFOSC spectrograph. The spectrum was reduced and analyzed as RES spectra.

All spectra were reduced to heliocentric velocities.

2.3. Infrared photometry

Infrared photometric observations were carried out at the ESO 1 m telescope in April 1984 and March-April 1985. We used an InSb photometer detector with $JHKLM$ filters. The integration times ranged from 45 seconds to 2 minutes depending on the filters and the selected signal to noise ratio. We used the following standard stars, extracted from the specific ESO Photometric Catalogue: HR 5132, HR 6748, HR 4167, HR 3314, HR 2970, HR 5824, HR 2845, HR 3842, HR 7120, HR 6736, HR 4695. JHKLM magnitudes were corrected for atmospheric extinction using the average ESO extinction coefficients.

2.4. Infrared spectrophotometry

Narrow band spectrophotometric observations were performed in the same period at the ESO 1 m telescope + InSb photometer + CVFs in order to give the energy distribution in the IR region up to 5 μm. The spectral resolving power was 70. The integration time for each filter was $30-45$ seconds. In order to obtain the measurements in the full range for each CVF, $5-30$ minutes were required. HR 2970, HR 4013, HR 5966 and HR 6748, extracted from the specific ESO Photometric Catalogue, were used as standard stars. The journal of observations is presented in Table 2.

The IR observations were almost simultaneous with the spectroscopic observations.

3. Results

3.1. Optical photometry

UBV photometry (Table 3), carried out in January 1996, shows that Z CMa is presently in a low state at $V = 10.24 \pm 0.01$. This value is in good agreement with the decreasing luminosity trend shown in the AAVSO database regarding Z CMa (Mattei 1996). We derived the following colors: $B-V = +1.00$ and $U-B = +0.54$.

3.2. Low-dispersion spectra

In the period March-April 1985 the star was in an active state, confirmed by the measured value $V = 9.0$, in comparison with $V = 9.4$ measured in April 1984 (Hessman et al. 1991). The variability trends of Hγ, Hβ, Hα and Fe II lines are shown in Fig. 1.

The main variations occurred from April 1984 to March-April 1985 are the following:

1. An increase of about 100% of the Hα emission line and an increase of 100 km s^{-1} of the velocity of its blue-shifted absorption component (Fig. 1, Tables 4 and 5),
2. An increase of the $FWHM$ width of the Hα emission from 6 to 8.6 Å, corresponding to an expansion velocity increase of about 120 km s^{-1} (Fig. 1, Table 5).
3. The transition of the Hβ line from a pure absorption profile to a strong P Cygni profile and an increase of 160 km s^{-1} of its blue-shifted absorption component (Fig. 1, Table 5).
4. A strong increase of Fe II emission number and the transient occurrence of strong P Cygni effects in some of the Fe II lines (Fig. 1, Table 6).

No significant variations are present in the Na I D doublet.

The spectrum obtained on January 17 1996 shows a very prominent variation of the state of the star, characterized by a drastic change of the Hα profile and by a 20% increase of Hα emission EW in comparison with the 1985 spectrum (Fig. 1, Table 4). The presence of some slight P Cygni effects both in Hβ and in Hγ seems to indicate a residual activity. A much more detailed analysis of the unusual Hα profile and of other peculiar characteristics was performed on the medium dispersion BFOSC spectrum, the results of which are discussed in Sect. 3.3.

No clear evidence of variability of EW and profile on a monthly or daily time scale is present in any spectrum.

A study of very short-term variability (seconds to minutes), carried out with a time-sequence of 15 spectra on April 16, 1984 and with a time-sequence of 7 spectra on April 17, 1984, gave a negative result: the most important lines (Hα and Hβ) did not show any EW or morphological variation. This result can be expected because of the quiescent state of the star in this period, in which friction-driven fast variations in the gas of the accretion disk are unlikely to be observed using low-dispersion spectroscopy. A study of the short-term variability could give more significant results in the active states of the star. Unfortunately we could not carry out this monitoring in 1985 due to the limited available observing time.

Table 4. Equivalent widths in Ångstrom of the Balmer lines and the doublet Na I D from IDS spectra. Typical errors are $\sim 20\%$

Date	Absorption				Emission		
	Hγ	Hβ	Na I	Hα	Hγ	Hβ	Hα
Apr. 84	3.7	5.8	6.9	2.8	0.7	absent	14.6
Mar. 85	4.3	3.9	5.2	3.2	0.3	2.4	24.9
Apr. 85	4.4	3.5	5.7	2.9	0.2	2.6	28.3
Jan. 96	1.1	2.9	5.7	absent	2.5	0.7	32.5

3.3. Medium and high-dispersion spectra

Our CASPEC spectrum on April 11, 1985 supplied the most detailed line analysis. As it is possible to see in Figs. 2, 3 and Table 7, the 15 reduced echelle orders present a great number of emission lines. The strongest P Cygni effect is present in Hα (Fig. 4), where we measured a heliocentric velocity $V_r = -510$ km s^{-1} from the

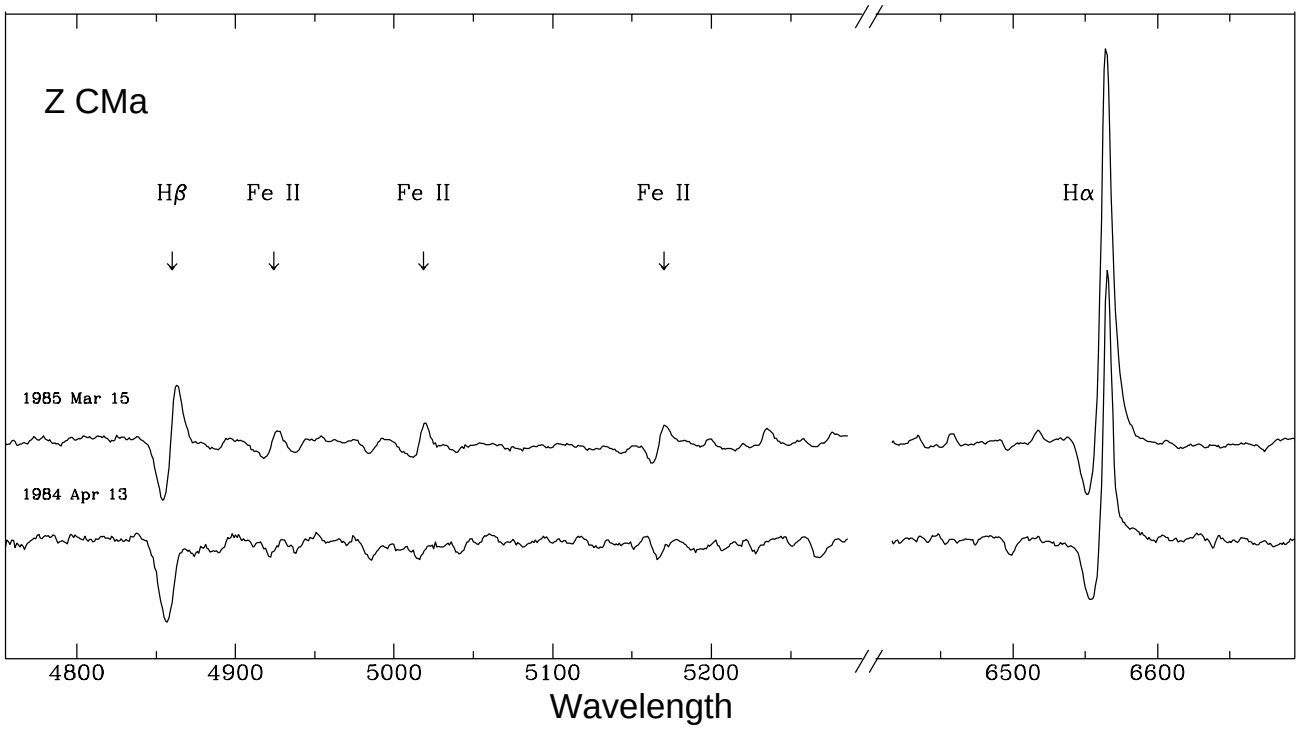

Fig. 1. Variation of the Z CMa spectrum from the 1984 quiescent state to the 1985 active state (IDS spectra). Transition of Hβ from pure absorption to P Cygni morphology, enhancement of Hα, and the appearance of Fe II emission are seen

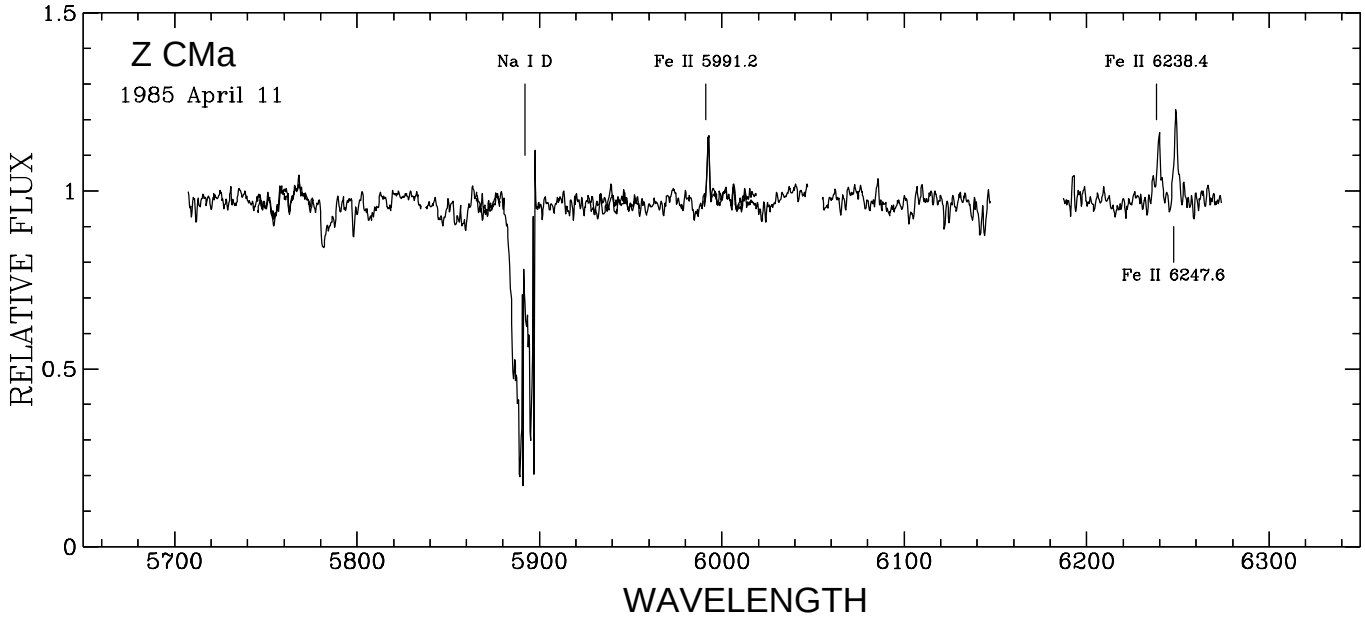

Fig. 2. CASPEC overall spectrum (5700 – 6250 Å) obtained during the 1985 active state. Identified lines are indicated

Table 5. Outstanding dynamical parameters of Hα and Hβ by IDS spectra

Date	*RV Hα (A) (km s^{-1})	$FWHM$ Hα (E) (Å, km s^{-1})	*RV Hβ (A) (km s^{-1})
1984 Apr. 13	− 486.37	6.04, 276.21	− 334.97
1985 Mar. 15	− 582.03	8.60, 393.17	− 493.23

A: Absorption, E: Emission
* RV heliocentric.

Table 6. Emission lines other than Balmer present in low-dispersion spectra

	Present at Days of Months:			
Identification	Apr. 84	Mar. 85	Apr. 85	Jan. 96
Fe II 4923.92	-	15, 16, 17	8, 9	17
Fe II 5018.43	-	15, 16, 17	8, 9	17
Fe II 5158.00	14	-	-	-
Fe II 5169-71	-	15	9, 10	17
Fe II 5199.20	-	-	9, 10	-
Fe II 5234.62	-	15, 17	9, 10	-
Fe II 5269.54	-	15, 17	9, 10	-
Fe II 5276.00	-	15, 17	9, 10	-
Fe II 5284.09	13, 14, 15	15, 17	9, 10	-
Fe II 5316.61	-	15, 17	9, 10	17
Ti II 5336.80	-	-	9, 10	-
Fe II 5362.86	13, 14, 15	15, 17	9, 10	-
Fe II 5534.90	-	15, 17	9, 10	-
Fe II 6149.71	-	15, 17	9, 10	-
Fe II 6238.38	-	15, 17	9, 10	-
Fe II 6247.56	-	15, 17	9, 10	-
[O I] 6300.20	-	15, 17 (W)	9 (W)	17 (S)
Fe II 6369.50	-	-	-	17
Fe II 6432.65	-	15, 17	9, 10	17
Fe II 6456.38	-	15, 17	9, 10	-
Fe II 6516.05	-	15, 17	9, 10	
Fe II 6627.30	13	-	-	-
[S II] 6717.00	-	-	-	17
Fe II 6729.90	-	-	-	17
Fe II 7155.10	-	-	-	17
Fe II 7376.50	-	-	-	17

W: Weak, S: Strong.

absorption component. The velocity difference between the Hα emission and absorption components is on the order of 550 km s^{-1}, while the blue wing of the Hα absorption component is characterized by a terminal velocity of about 900 km s^{-1}. The doublet Na I D presents many absorption components (Fig. 5): the deepest one has $V_r = -52$ km s^{-1}, the bluest one has $V_r = -234$ km s^{-1}, extending up to a terminal velocity of 550 km s^{-1} (see also Table 7). Similar values can be deduced from the CES spectrum. Other P Cygni features can be seen in all Fe II lines but their absorption components are too weak to allow accurate equivalent width (EW) and radial velocity (RV) measurements. Much stronger P Cygni effects, as easily shown in the 1985 low-dispersion spectra, should have appeared in the range 4900 − 5200 ÅÅ in Fe II 4923 Å, 5018 Å and 5169 − 71 ÅÅ lines, but unfortunately this range was not covered by CASPEC spectra. The average velocity of the Fe II absorption components is −90 km s^{-1} while the average velocity of the Fe II emissions is about 38 km s^{-1}, comparable with the average velocity of the Hα emission component (+46 km s^{-1}).

In addition to emission and P Cygni features, CASPEC spectra show clear evidence of double-peaked absorption lines at $\lambda\lambda$ 5915 Å, 6142 Å, 6192 Å, 6440 Å, 6451 Å, 6496 Å, 6644 Å, 6678 Å, 6664 Å, 6709 Å and 6719 Å: we measured an average velocity of their peak separation $V_s = 119 \pm 4$ km s^{-1}. The absorption line He I 6678.15 Å, blended with the Fe I disk doubled absorption line at 6678 Å (Fig. 6), apparently is the only photospheric feature of interest in our CASPEC spectra. A blue-shift corresponding to $V_r = -207$ km s^{-1} was derived for the He I 6678.15 Å absorption line.

Our CES spectra (Fig. 7, Table 8) were mostly concentrated on Hα. No relevant monthly EW variation of the Hα emission is detected between the spectra taken on April 8–9, 1985 and the spectrum taken on March 15, 1985. The EW's may be affected by an erroneous determination of the continuum level due to the small spectral range covered by CES spectra. At the same time, some differences are evident in absorption components between the March and April spectra.

From CES spectra we determine an average velocity of −470 km s^{-1} for the Hα absorption component and an average velocity of +44 km s^{-1} for the emission component. There is a velocity decrease of about 20 km s^{-1} from 15 March to 8–9 April, which we interpretate as a consequence of wind deceleration. Furthermore, CES spectra show also very strong Ca II 8498 Å and 8542 Å emission, whose radial velocities seem to be in good agreement with the Hα emission measurement. Ca II lines are present with a (more or less) pronounced P Cygni profile. The derived velocities from absorption components are −116 and −196 km s^{-1} respectively. This difference can be interpreted as the effect of two equally dense and hot shells ejected at different velocities.

The small difference between the velocities measured with CES and the ones measured with CASPEC is probably due to the fact we used two different instruments. Because of this, we focus attention on measurements made with a single instrument and consequently to ratios obtainable between values of a given line parameter present in a specific spectrum.

From the medium-dispersion spectra taken with the RES spectrograph, we obtained Hα (Fig. 4) and Hβ profiles. The emissiony (EW = 15.48 Å) and absorption (EW = 6.42 Å) components of Hα show a velocity difference of 656 km s^{-1}, while the blue wing of the absorption component extends out to −1150 km s^{-1}. Hβ is present strongly in absorption (EW = 7.00 Å) with a weak emission component (EW = 0.10 Å), absorption and emission components show a velocity difference of 270 km s^{-1}.

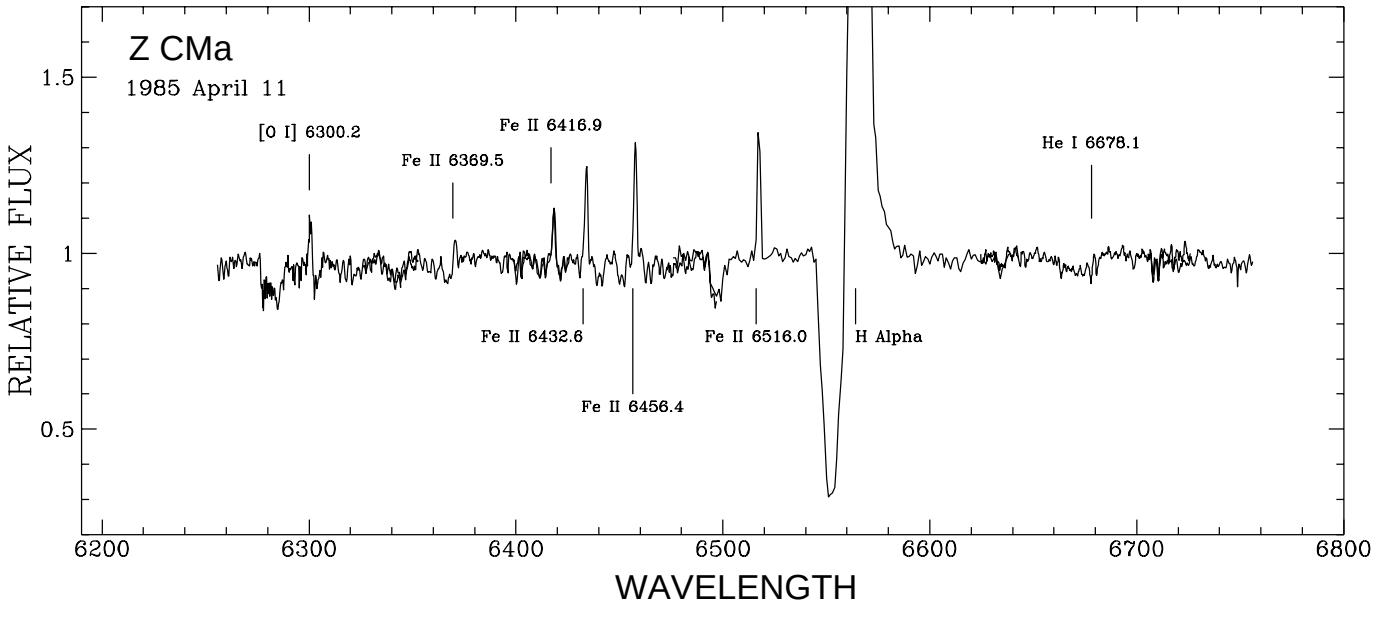

Fig. 3. CASPEC overall spectrum (6250 − 6750 Å) obtained during the 1985 active state. Identified lines are indicated

BFOSC spectra (Table 9 and Figs. 8 and 9) obtained with a medium-dispersion of 22 Å/mm show the most interesting characteristics both in terms of variability and in terms of peculiar morphology. The following fundamental features are evident:

1. The Hα profile is completely changed in comparison to the profile shown in the 1984–1985 spectra (Fig. 4). In addition to the main emission a second blue shifted emission is present. The central absorption, shifted by -516 km s^{-1} with respect to the main emission, corresponds perfectly to the absorption detected in the ESO spectra. The central wavelengths of the two Hα emission components are separated by a velocity of over 800 km s^{-1}.

2. The spectrum shows the usual Fe II emissions which are normally present in the spectrum of Z CMa during the active states, but only the Fe II 5169 Å line shows a sharp P Cygni effect. All the other Fe II lines do not show P Cygni features. The average velocity of the Fe II emissions is $+77$ km s^{-1}.

3. The spectrum shows the forbidden [O I] 6300 Å emission line (EW = 1.5 Å), much stronger than in the 1985 CASPEC spectrum, and the forbidden [S II] 6717 Å (EW = 0.1 Å), [S II] 6731 Å (EW = 0.5 Å) and [Fe II] 7155 Å (EW = 0.4 Å) emission lines. In particular, [O I] 6300 Å and [S II] 6731 Å present both an asymmetric profile with the red component much stronger than the blue, and with barycenters strongly blue-shifted.

4. The blue wing of the Na I 5889.9 Å absorption line corresponds to a velocity of over -470 km s^{-1}, about 80 km s^{-1} less than the values derived from April 1985 CASPEC and CES spectra.

5. In five cases, at 6192 Å, 6345 Å, 6496 Å, 6644 Å and 6664 Å, we identified double-peaked "disk absorption lines". An average velocity of 115 ± 6 km s^{-1} was obtained from their peak separation. The shallow He I 6678 Å absorption line, present in CASPEC 1985 spectrum, is absent. At the same wavelength the BFOSC spectrum shows a strong double peaked "disk absorption line".

3.4. IR photometry

As shown in Table 10, $JHKLM$ photometry shows decreases of up to $0.2 - 0.3$ mag from April 1984 to March-April 1985. In the same period, color indexes $J-K$, $H-K$ and $K-L$ are subject to a blueing effect consistent with a decrease of up to 0.2, 0.08 and 0.08 mag respectively. We notice that such IR luminosity increases and color blueing can be correlated with analogous variations detected in the optical range (Hessman et al. 1991). Similar variations in the IR range can be found in the literature (Kenyon & Hartmann 1991; Berrilli et al. 1992; Hamann & Persson 1992; Molinari et al. 1993; Noguchi et al. 1993). No luminosity or blue increases larger than $0.02 - 0.06$ mag are recorded on a daily or monthly timescale.

3.5. Energy distribution

The energy distributions in the range 0.4−5 μm obtained in 1984 and 1985, are presented in Fig. 10. The optical components of these distributions are represented by low-dispersion spectra taken on March 17, 1985 and on April 17 1984. The IR components are given by an average of spectrophotometric data taken in March and April 1985, overlapped with IR photometric data taken in April 1984 and April 1985.

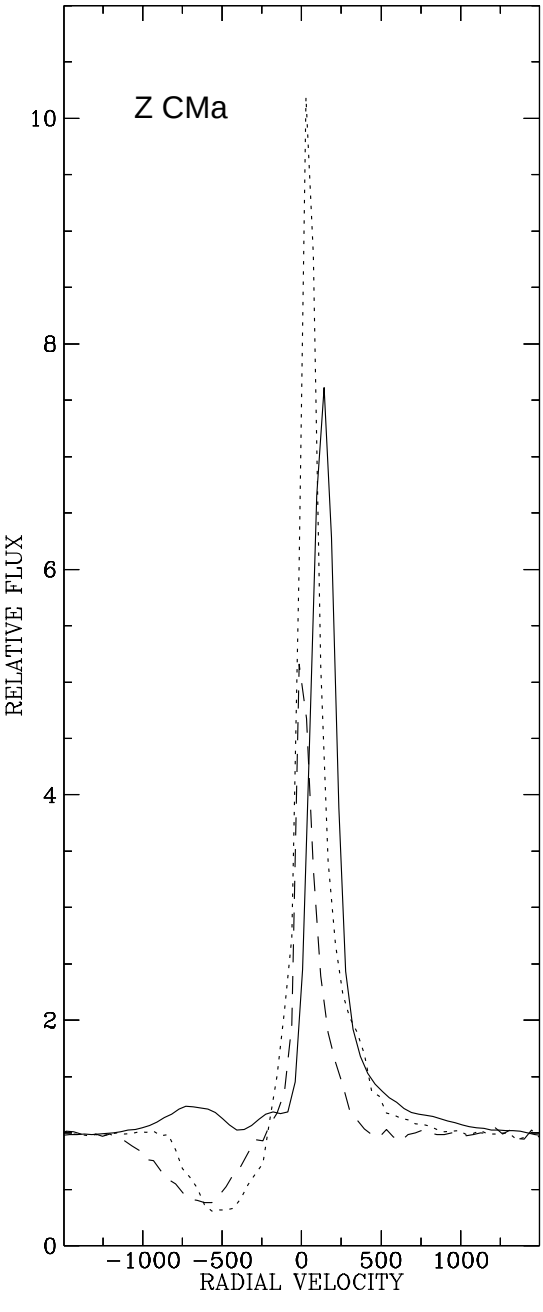

Fig. 4. Hα line in 1985 CASPEC spectra (short dash), 1989 REOSC spectra (long dash) and 1996 BFOSC spectra (solid). Radial velocity (km s^{-1}) is heliocentric

The following main features can be outlined from the energy distributions:

1. The distributions peak around 1.6 μm.
2. A deep absorption band, at about 1.9 μm.
3. The increase of the 1985 IR flux with respect to that of 1984, by a factor of 1.4 in the J passband, 1.3 in H, 1.2 in K and 1.1 in L and M.

The absorption band at 1.9 μm, due to the composite transitions of vibration-rotation bands of water vapor

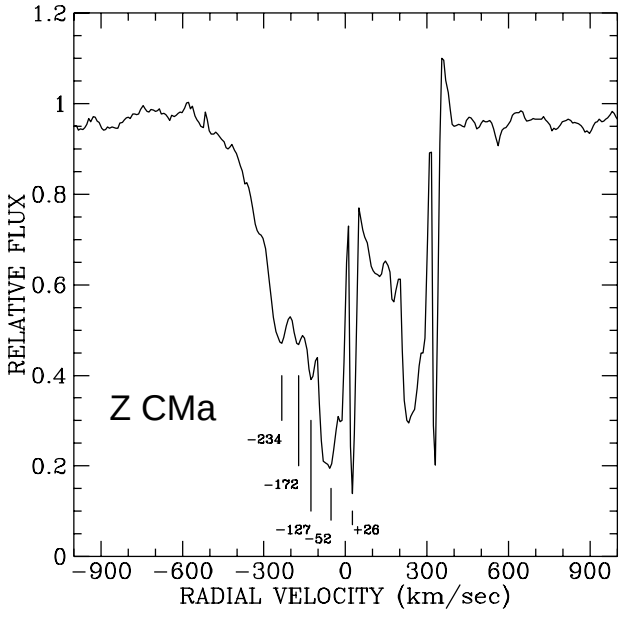

Fig. 5. Absorption components of doublet Na I D (CASPEC spectrum acquired in 1985 April 11). Heliocentric velocities (km s^{-1}) of absorption components of Na I 5889.9 Å are indicated

(Sato et al. 1992), is the only clear and seemingly constant characteristic of the IR spectrophotometric energy distribution. This absorption feature is the result of the heating effect on water-ice grains which are contained in the external region of the proto-stellar accretion disk. Such heating is caused by the ionization front developed during the 1985 phase.

Given the variability of Z CMa, different energy distributions are expected from data taken in different epochs. In particular, in our data this difference can be noticed in the general flux increase from 1984 to 1985, in a steep increase in the J and H fluxes and in the basic equality of H and K fluxes of 1985 (in comparison with 1984 IR data).

Previous authors (Berrilli et al. 1992; Natta et al. 1993) demonstrate that the envelope is the source of a strong IR excess starting at about 2 μm.

4. Discussion

Our observations show three well distinguished states of Z CMa.

4.1. The 1984 and 1989 quiescent states

In April 1984 the star was in a quiescent state mainly characterized by $m_V = 9.7$ (Mattei 1996) and by the absence of emission components in the Hβ and Fe II line profiles. In October 1989 Z CMa was in a semiquiescent state characterized by $m_V = 9.6$ (Mattei 1996) and by the presence of very weak Hβ and Fe II 4923.9 emission components.

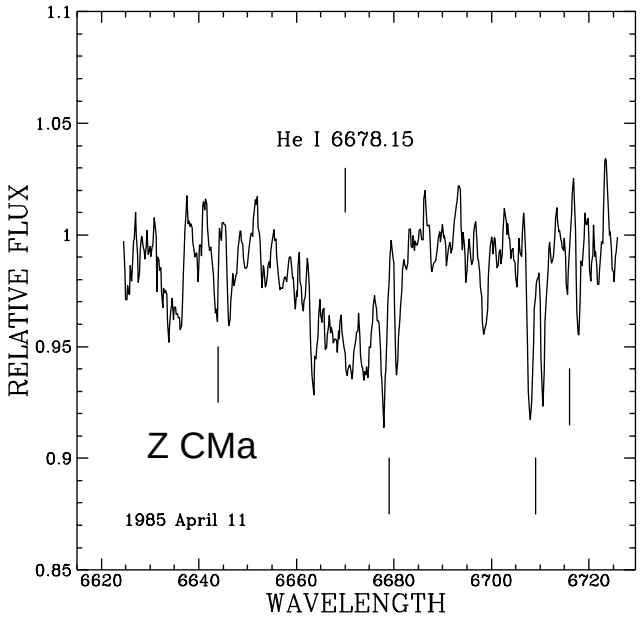

Fig. 6. CASPEC spectrum (1985 April 11) showing He I 6678.15 deep absorption line. Double-peaked absorption lines at 6644, 6679, 6709 and 6719 Å are also indicated

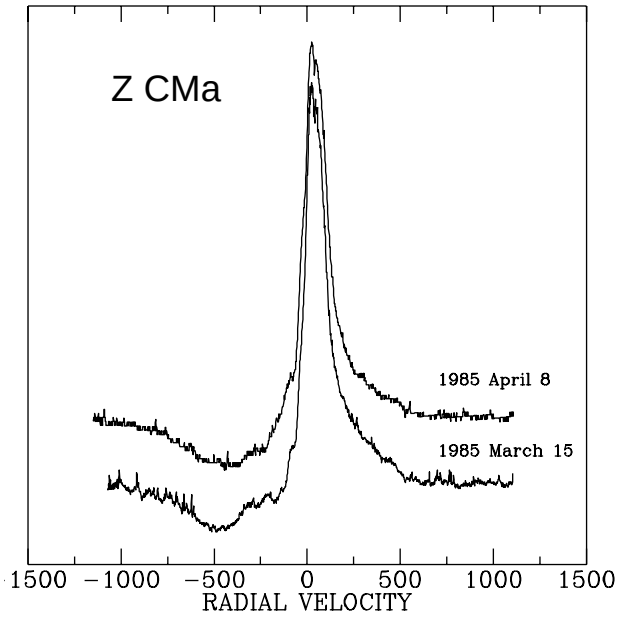

Fig. 7. CES spectra, obtained during the 1985 active state, showing variation of the Hα absorption component within a period of approximately a month

The extension out to -1150 km s^{-1} of the blue wing of the Hα absorption component still indicates the presence of a strong wind with a terminal velocity comparable to the post-eruption one (Hessman et al. 1991).

4.2. The 1985 active state

In March–April 1985 we record an increase of 0.2–0.3 mag in the $JHKLM$ bands and our low-dispersion spectra show the transient occurrence of Fe II line emissions (in particular, the 5169 Å line with a strong P Cygni profile), a strong enhancement of the Hα line and a sharp transition of Hβ from a pure absorption to a strong P Cygni profile, and finally the increase of over 100 km s^{-1} of the blue shifted absorption component of the most prominent P Cygni lines. Our data allow us to compare the behaviour of Z CMa in the quiescent-active transition state (April 1984 - March 1985) to the active-quiescent transition state (February 1987 – December 1988) described by Hessman et al. (1991). Thus we are able to confirm that the active state of the star is characterized by a strong enhancement of the outflow power, as strongly indicated by the increase of both the EW and $FWHM$ of the Hα emission component and the RV of the Hα absorption component.

The blue-wing extensions of the absorption components of the most prominent P Cygni lines present in the April 1985 spectra have velocities of $200 - 300$ km s^{-1} less than the values measured by Hessman et al. (1991) during the 1987 outburst. For this reason, and taking into account also the coeval low-dispersion data, we find that

Table 7. Equivalent widths (EW) and radial velocities (RV) of prominent lines present in CASPEC spectra acquired on April 11 1985. Error in EW is $5 - 10\%$, error in RV is $2 - 5\%$. Four values of RV are measured for Na I D corresponding to different components as shown in Fig. 5, while the given EW is the total

Identification	Absorption		Emission	
	EW (Å)	RV** (km s^{-1})	EW (Å)	RV** (km s^{-1})
Na I D	7.0	− 52		
″		− 127		
″		− 172		
″		− 234		
″		+ 26*		
Fe II 5991.4	0.2	− 69	0.2	+ 40
Fe II 6238.4	weak	− 66	0.5	+ 37
Fe II 6247.6	weak	− 119	0.6	+ 40
[O I] 6300.2			0.2	− 2.4
Fe II 6369.5	weak	− 74	0.1	+ 25
Fe II 6416.9	weak	− 144	0.2	+ 38
Fe II 6432.6	weak	− 105	0.4	+ 45
Fe II 6456.4	weak	− 72	0.5	+ 37
Fe II 6516.0	weak	− 84	0.7	+ 38
Hα	6.5	− 510	29.1	+ 46
He I 6678.1	1.0	− 207		
Fe II 6729.9			0.1	+ 20

* Interstellar line
** RV heliocentric.

Table 8. Equivalent widths (EW) and radial velocities (RV) of prominent lines present in CES spectra. Error in EW is $5-10\%$, error in RV is $2-5\%$

Identification	Absorption		Emission		Date
	EW (Å)	RV** (km s^{-1})	EW (Å)	RV** (km s^{-1})	
Na I D	3.5	− 51 *			Mar. 16
Hα	4.5	− 483	15.8	+ 44	Mar. 16
〃	5.5	− 465	15.7	+ 45	Apr. 8
〃	5.2	− 467	15.8	+ 46	Apr. 9
Ca II 8498.0	0.2	− 116	4.6	+ 38	Apr. 10
Ca II 8542.1	0.5	− 196	5.2	+ 47	Apr. 10

* Deepest component
** RV heliocentric.

Table 9. Prominent lines present in BFOSC (22 Å mm^{-1}) spectra acquired on January 17 1996. Error in EW is $5-10\%$, error in RV is $4-5\%$. For lines with $\lambda < 5460$ Å it was not possible to measure RV because of bad calibration due to echelle order overlapping

Identification	Absorption		Emission	
	EW (Å)	RV* (km s^{-1})	EW (Å)	RV* (km s^{-1})
Fe II 5169.0	0.3		0.3	
Fe II 5284.1			0.4	
Fe II 5455.6?	0.4		0.2	
Hg I 5460.7?			0.3	+ 5.6
Na I D	5.4	− 40		
[O I] 6300.2			1.5	− 214
Fe II 6432.6			0.2	+ 87
Fe II 6456.4			0.2	+ 97
Fe II 6516.0			0.3	+ 116
Hα	1.0	− 378	2.3	− 677
〃			32.5	+ 138
[S II] 6717.0			0.1	− 6.0
[S II] 6731.3			0.5	− 102
[Fe II] 7155.1			0.4	+ 35
Fe II 7376.5			0.5	+ 48
O II 7938.1?				
O I 8446.4			1.5	+ 52
Ca II 8498.0			5.6	+ 68
Ca II 8542.1	0.3	− 154	6.4	+ 75
Ca II 8662.1	0.1	− 173	5.4	+ 60

* RV heliocentric.

the state of Z CMa in April 1985 was characterized by a small eruption.

Moreover, the presence of He I 6678 Å absorption line, mixed with double-peaked "disk absorption lines", further confirms that, in 1985, Z CMa was in a much less active state than the one recorded in 1987, in which absorption disk-lines were almost absent in the region 6610−6740 ÅÅ, while a veiling effect, together with a strong He I 6678 Å line, was observed (Hessman et al. 1991). Finally, from the peak separation of the few disk-lines at our disposal, we measured a velocity lower than that measured in 1987. Therefore, in 1985 the accretion disk of Z CMa was crossing an intermediate stage of the shrinkage process and of the consequent keplerian rotation rate.

In general, the appearance of a photospheric line such as He I 6678 Å demonstrates that, during the active states of Z CMa, a stellar wind driven by the central star is overlapped with an outflow, as evidenced by P Cygni lines, driven by the accretion disk.

Considering the "mini-eruption phenomenology" as a whole, we notice that the object Z CMa, capable of long-duration and very low-frequency outbursts up to 3 magnitudes in amplitude, possesses additional and important explosive characteristics, consisting in small-amplitude and short-duration eruptions which coexist with the big outbursts. For this reason we suggest that Z CMa has properties of both a FUOr object and an EXOr object. EXOrs are more evolved proto-stars which are characterized by small-duration (~ 1 yr), small-amplitude ($0.4-1.0$ mag) and high-frequency (few years) eruptions (Hartmann et al. 1993): this seems to indicate that accretion disk thermal instability processes decrease in intensity and increase in frequency as the object approaches the ZAMS. Perhaps Z CMa could be a serendipitous example of a link between the FUOr phase and the EXOr phase. For this reason, we stress the importance of developing further models regarding both stellar evolution and accretion disk thermodynamics.

4.3. The 1996 new state

The most relevant aspects of Z CMa's behaviour in 1996 are the following:

1. The star is at a low-level luminosity ($V = 10.24$), with a red $U-B$ color typical of post-outburst states but with a $B-V$ color bluer than typically measured in post-outburst states ($B-V = 1.15-1.20$). The blueing of $B-V$ could be due to a decreased extinction of the central star due to a strong decrease of the circumstellar envelope density. A $B-V$ color change due to a shrinkage process of the accretion disk could be an alternative possibility as well, but we consider it unlikely as it would be inconsistent with the low value of the velocity of double-peaked disk absorption lines and with the missing transition of the spectrum toward an earlier type (absence of He I 6678 Å absorption line). The value (115 km s^{-1}) inferred from our double-peaked absorption lines, compared with the value (110 km s^{-1}) typical of the post-eruption low state (Hessman et al. 1991), together with the total absence of He I 6678 Å absorption line, proves in fact the existence of a semi-low state of Z CMa in January 1996.

2. The Hα profile is completely changed from a pure P Cygni profile to a composite profile which seems to be a mix of a P Cygni and of a double emission profile. We think that this combination, never encountered before in the relevant literature on Z CMa, might be the consequence of a significant and possibly asymmetrical increase

Table 10. $JHKLM$ photometric data

Date	J.D.	J	H	K	L	M
1984 Apr. 17	2445807.558	6.11±.03	4.84±.01	3.68±.01	1.85±.06	0.93±.10
1984 Apr. 18	2445808.551	6.15 .03	4.88 .04	3.71 .04	1.90 .10	0.94 .15
1985 Mar. 17	2446141.507	5.82 .02	4.61 .03	3.52 .01	1.76 .04	0.80 .06
″	2446141.666	5.80 .02	4.65 .03	3.52 .01	1.73 .04	0.77 .06
1985 Mar. 18	2446142.579	5.81 .02	4.63 .02	3.53 .01	1.75 .03	0.83 .05
1985 Apr. 9	2446164.546	5.84 .02	4.70 .03	3.60 .02	1.83 .03	0.85 .15
1985 Apr. 10	2446165.499	5.78 .04	4.66 .04	3.56 .02	1.81 .02	0.87 .18
1985 Apr. 11	2446166.490	5.83 .04	4.68 .03	3.59 .03	1.81 .03	0.83 .07
″	2446166.497	5.82 .04	4.66 .03	3.56 .03	1.79 .03	0.80 .07
″	2446166.516	5.82 .04	4.67 .03	3.56 .03	1.79 .03	0.80 .07
″	2446166.523	5.81 .04	4.66 .03	3.57 .03	1.81 .03	0.79 .07

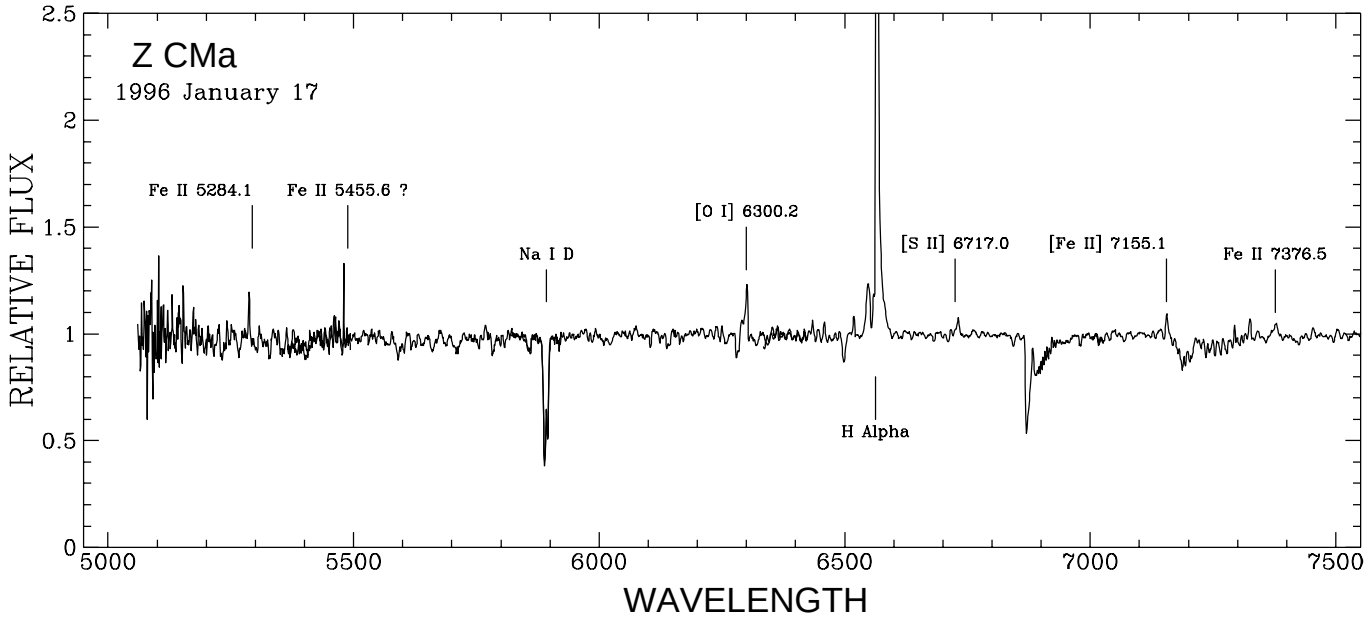

Fig. 8. BFOSC overall spectrum (5000 − 7500 Å) obtained in 1996 January 17. Identified lines are indicated

of the opening angle of the outflow. If this is the case, it could be expected that the blue-shifted small emission is produced, via mechanical gas heating, in the optically thin approaching part of the outflow where the line emission is restricted to the volume outside the surface of an asymmetric hollow cone or paraboloid. If one assumes that such an increase of the outflow opening angle really occurs, one can expect a general gas rarefaction as well. Such an effect could produce evidence of an optically thin and very extended outflow where forbidden lines can be found. In fact we record [O I] 6300 Å and [S II] 6731 Å forbidden lines.

Finally, the red region of the spectrum is characterized by the presence of strong emissions due to O I and Ca II.

3. The star shows a residual activity, which can be inferred from the high value of the Hα emission EW, from the presence of Fe II emissions, of faint P Cygni profiles at Hγ, Hβ (Fig. 2), and at Ca II 8542 − 8662 Å lines. The reason for such residual activity is, at the present time, not clearly understood.

5. Conclusions

In summary, the spectroscopic and photometric variations observed in 1985 show the transition of the star from a quiescent state to an active state. Our data confirm the results of the observations of previous authors.

In particular our spectra clearly show that the 1985 state has a lower level of activity with respect to the one observed in 1987.

In 1989 Z CMa returned to approximately the 1984 brightness level, but the spectrum still shows evidence of residual activity.

The most important result of our spectroscopic observations of Z CMa is given by the very peculiar profile change of H_α observed in January 1996. The appearance of a double emission profile might be explained by geometric

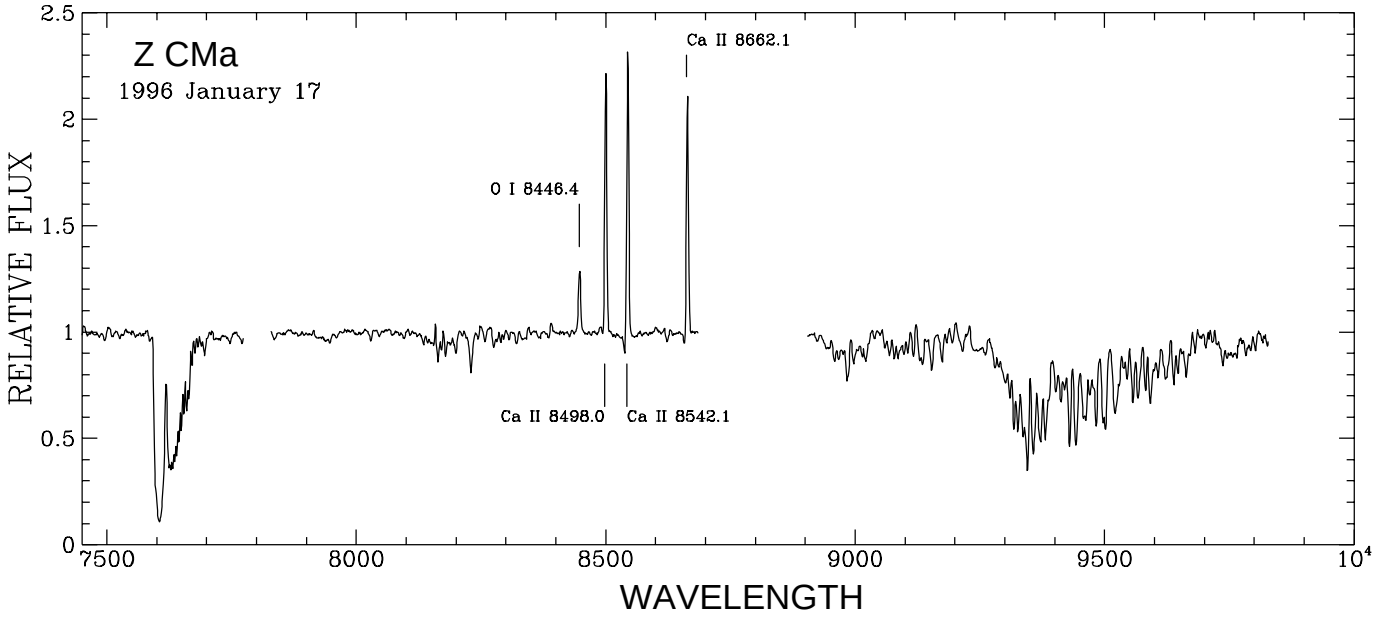

Fig. 9. BFOSC overall spectrum (7500 − 9800 Å) obtained in 1996 January 17. Identified lines are indicated

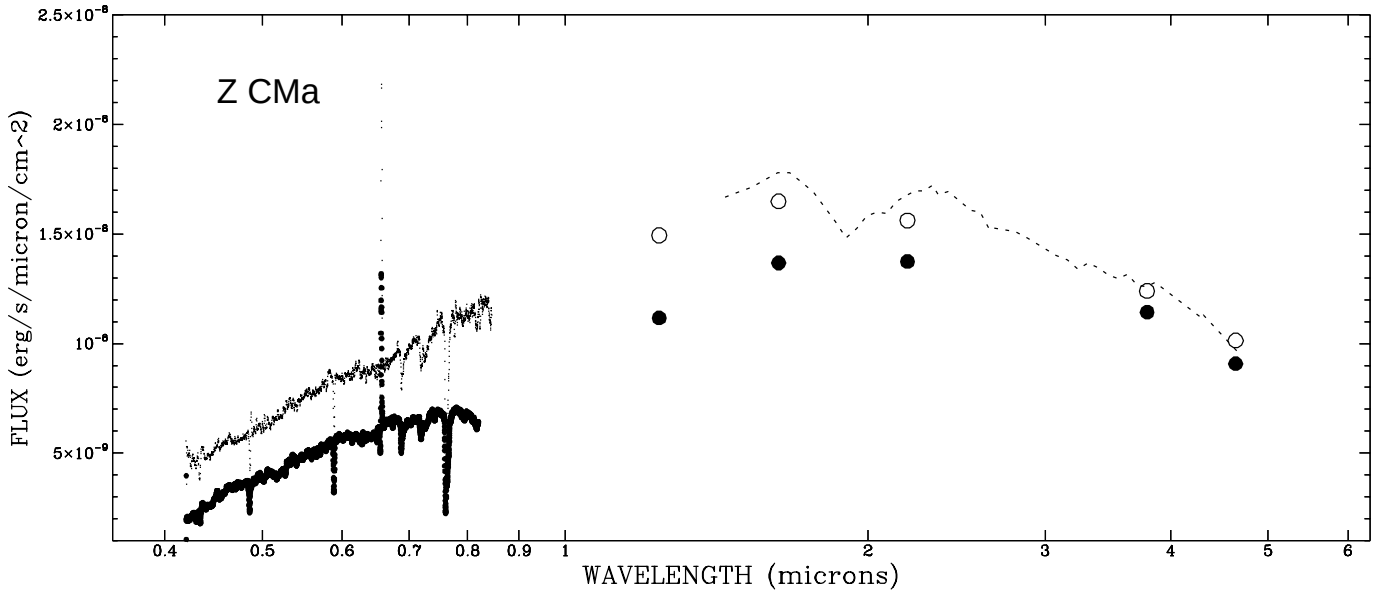

Fig. 10. Energy distribution of Z CMa in the range $0.4 - 5$ μm constructed from April 1984 (thick line) and March 1985 (dotted line) spectroscopic data merged with IR March-April 1985 spectrophotometric data (dashed line), IR April 1984 photometric data (filled circles) and IR April 1985 photometric data (open circles)

effects due to variation of the opening angle of the bipolar outflow. Furthermore a strong decrease of the circumstellar envelope density may explain the observed decrease in the $B - V$ index.

Further and higher dispersion spectroscopy is proposed for the future in order to allow a much more detailed description of possible geometric effects causing the peculiar morphology of the Hα emission line profile.

Acknowledgements. We are indebted to Dr. J.A. Mattei who provided us with photometric observations of Z CMa in the period 1976–1996. We thank Dr. Krautter for allowing us to obtain the CASPEC spectrum. We are indebted to Prof. A. Guarnieri of Bologna Astronomy Department for giving us precious help with BFOSC observations at the Loiano 1.52 m telescope. We wish to thank also Dr. Kevin Reardon for carefully reading our manuscript.

References

Berrilli F., Corciulo G., Ingrosso G., et al., 1992, ApJ 398, 254
Bhatt H.C., Sagar R., 1992, A&AS 92, 473
Covino E., Terranegra L., Vittone A.A., Russo G., 1984, AJ 89, 1868
Croswell K., Hartmann L., Avrett E.H., 1987, ApJ 312, 227
Hamann F., Persson S.E., 1992, ApJ 394, 628
Hartmann L., Kenyon S.J., Hewett R., et al., 1989, ApJ 338, 1001
Hartmann L., Kenjon S., Hartigan P., 1993, in "Protostars and Planets III", Levy E.H., Lunine J.I. (eds.). The University of Arizona Press, p. 497
Hartmann L., Calvet N., 1995, AJ 109, 1846
Herbig G.H., 1960, ApJS 6, 337
Herbst W., Booth J.F., Koret D.L., et al., 1987, AJ 94, 137
Hessman F.V., Eislöffel J., Mundt R., et al., 1991, ApJ 370, 384
Kenyon S.J., Hartmann L.W., 1991, ApJ 383, 664
Koresko C.D., Beckwith S.V.W., Ghez A.M., Matthews K., Neugebauer G., 1991, AJ 102, 2073
Mattei J.A., 1996, Observations from the AAVSO International Database (private communication)
Merrill P.W., 1927, ApJ 65, 291
Miroshinenko A.S., Yudin R.V., Shejkina T.A., Turdaliev B., 1993, IBVS 3937
Molinari S., Liseau R., Lorenzetti D., 1993, A&AS 101, 59
Natta A., Palla F., Evans II N.J., Harvey P.M., 1993, ApJ 406, 674
Noguchi K., Quian Z., Wang G., Wang J., 1993, PASJ 45, 65
Oudmaijer R.D., Van der Veen W.E.C.J., Waters L.B.F.M., et al., 1992, A&AS 96, 625
Poetzel R., Mundt R., Ray T.P., 1989, A&A 224, L13
Pickering E.C., 1913, HCO Circ., 178
Sato S., Okita K., Yamashita T., et al., 1992, ApJ 398, 273
Strom S.E., Strom K.M., Yost J., Carrasco L., Grasdalen G., 1972, ApJ 173, 353
Torres C.A.O., Quast G., De la Reza R., Gregorio-Hetem J., Lepine J.R.D., 1995, AJ 109, 2146
Welty A.D., Strom S.E., Edwards S., Kenyon S.J., Hartmann L.W., 1992, ApJ 397, 260